iPS Cell-Derived Dopamine Neurons Reveal Differences between Monozygotic Twins Discordant for Parkinson's Disease

Chris M. Woodard[1,10], **Brian A. Campos**[1,10], **Sheng-Han Kuo**[2,10], **Melissa J. Nirenberg**[3], **Michael W. Nestor**[1], **Matthew Zimmer**[1], **Eugene Mosharov**[2], **David Sulzer**[2], **Hongyan Zhou**[1], **Daniel Paull**[1], **Lorraine Clark**[4], **Eric E. Schadt**[5], **Sergio Pablo Sardi**[6], **Lee Rubin**[1,7], **Kevin Eggan**[1,7,8], **Mathew Brock**[9], **Scott Lipnick**[1], **Mahendra Rao**[1], **Stephen Chang**[1], **Aiqun Li**[1,*], and **Scott Noggle**[1,*]

[1]The New York Stem Cell Foundation Research Institute, New York, NY 10032, USA

[2]Department of Neurology, Columbia University, New York, NY 10032, USA

[3]Department of Neurology, New York University Langone Medical Center, New York, NY 10016, USA

[4]Department of Pathology and Cell Biology, Columbia University, New York, NY 10032, USA

[5]Department of Genetics and Genomic Sciences, Icahn School of Medicine at Mount Sinai, New York, NY 10029, USA

[6]Genzyme Corporation, a Sanofi Company, Framingham, MA 01701, USA

[7]Department of Stem Cell and Regenerative Biology, Harvard University, Cambridge, MA 02138, USA

[8]The Howard Hughes Medical Institute, Harvard Stem Cell Institute, Stanley Center for Psychiatric Research, Harvard University, Cambridge, MA 02138, USA

[9]Axion Biosystems, 1819 Peachtree Road, Suite 350 Atlanta, GA 30309, USA

SUMMARY

Parkinson's disease (PD) has been attributed to a combination of genetic and non-genetic factors. We studied a set of monozygotic twins harboring the heterozygous *glucocerebrosidase* mutation

*Correspondence should be addressed to: Scott Noggle Ph.D., Tel: 212-851-5422, Fax: 212-851-5423, SNoggle@NYSCF.org. Aiqun Li Ph.D., Tel: 212-851-5422, Fax: 212-851-5423, Ali@NYSCF.org.
[10]Co-first author

(*GBA* N370S) but clinically discordant for PD. We applied induced pluripotent stem (iPS) cell technology for PD disease modeling using the twins' fibroblasts to evaluate and dissect the genetic and non-genetic contributions. Utilizing fluorescence-activated cell sorting, we obtained a homogenous population of 'footprint-free' iPS cell-derived midbrain dopaminergic (mDA) neurons. The mDA neurons from both twins had ~ 50% GBA enzymatic activity, ~ 3-fold elevated α-synuclein protein levels, and a reduced capacity to synthesize and release dopamine. Interestingly, the affected twin's neurons showed an even lower dopamine level, increased monoamine oxidase B (MAO-B) expression, and impaired intrinsic network activity. Overexpression of *wild-type* GBA and treatment of MAO-B inhibitors normalized α-synuclein and dopamine levels, suggesting a combination therapy for the affected twin.

INTRODUCTION

Monozygotic (MZ) twins exhibit marked phenotypic similarities due to their shared genetic makeup. Twin studies have been valuable for dissecting complex gene-environmental interactions in neurodegenerative disorders. In a study of twins in the United States, the concordance of MZ twins developing Parkinson's disease (PD) is 15.5%, whereas the concordance of dizygotic (DZ) twins is 11.1% (Tanner et al., 1999). A twin study in Sweden found a concordance rate for PD was 11% in MZ pairs and 4% for DZ pairs (Wirdefeldt et al., 2011). This demonstrates that PD is moderately heritable, in agreement with observations that familial PD cases are relatively uncommon (~10%) and that even monogenic forms of PD have reduced penetrance. We recently recruited a pair of MZ twins discordant for PD five years after diagnosis of the affected twin. The presented work details our efforts to evaluate the genetic and epigenetic insults that might potentially explain the discordant onset of PD in twins.

Homozygous or compound heterozygous *glucocerebrosidase (GBA)* mutations cause Gaucher disease, a lysosomal storage disorder. Recently, *GBA* mutations have been linked to a five-fold greater risk of developing Parkinsonism than non-carrier individuals (Sidransky et al., 2009) and are the most common genetic risk factor for PD to date. In *GBA*-PD patients, the clinical phenotypes are similar to those of idiopathic PD cases, except for the occurrence of more severe non-motor symptoms, particularly cognitive decline. Post-mortem examination of *GBA*-PD patients shows α-synuclein pathology (i.e. Lewy bodies) with a loss of dopaminergic neurons in the substantia nigra. *GBA* mutations might potentially lead to PD pathology by increasing αsynuclein aggregation (Mazzulli et al., 2011) or defective mitochondrial turnover (Osellame et al., 2013). It has been proposed that introduction of exogenous WT GBA could rescue these PD-related phenotypes (Cullen et al., 2011; Sardi et al., 2011). The penetrance of PD in *GBA* mutation carriers is approximately 30% by the age of 80, but a significant proportion of carriers will never develop PD during their lifetime (Anheim et al., 2012). It is unclear why a subset of *GBA* mutations carriers would develop PD whereas others do not. Evidence suggests that complex genetic and environmental factors confer the additional risks of PD development.

Induced pluripotent stem (iPS) cell technology offers a unique opportunity to study genetic and epigenetic risk factors present in patient-specific midbrain dopaminergic (mDA)

neurons compared to those from healthy controls. Dopaminergic neurons from genetic PD cases have been used to recapitulate relevant disease pathology, including αsynuclein accumulation, impaired dopamine (DA) release, mitochondrial dysfunction, vulnerability to oxidative stress, and increased ERK phosphorylation (Cooper et al., 2012; Devine et al., 2011; Jiang et al., 2012; Mazzulli et al., 2011; Nguyen et al., 2011; Reinhardt et al., 2013; Sanchez-Danes et al., 2012). Despite these findings, variability in differentiation efficiency and neuronal maturity pose major obstacles for PD disease modeling.

In this report, using iPS technology, we investigated the unique set of MZ twins and found that α-synuclein clearance is impaired in mDA neurons carrying *GBA* N370S regardless of disease status. Elevated monoamine oxidase B (MAO-B) level could in part explain the degree of impairment in DA production between mDA neurons derived from the MZ twins discordant for PD. Importantly, over-expression of GBA and inhibition of MAO-B activity rescued α-synuclein accumulation and DA release phenotypes. These results suggest that a 'multiple hit' process eventually contributes to reduced dopamine production, a pathology that could be rescued by a combination approach against α-synuclein and MAO-B.

RESULTS

Genetic Analysis Reveals the *GBA* N370S in the MZ Twins

We recently identified a pair of 68-year-old, MZ male twins of Ashkenazi Jewish background who are discordant for PD. The affected twin had been diagnosed with PD at age 63. His MZ twin has no signs or symptoms of Parkinsonism after detailed examination by a movement disorders specialist (Table S1). Short tandem repeats (STR) analysis confirmed that they are monozygotic (Fig. S1A). We screened their skin fibroblasts for 66 known PD genetic mutations (Marder et al., 2010). Both twins were found to carry heterozygous *GBA* N370S, an established genetic risk for PD. Whole exome sequencing (WES) of fibroblasts displayed that ~ 39,300 single nucleotide variants (SNVs) were called and 96% of SNVs were shared in both pairs (Fig. 1A, Table S2). Cross-referencing with the PD gene databases (Do et al., 2011; Lill et al., 2012), we identified 82 PD-related SNVs (Table S3). Among these variants, *GBA* N370S exhibited a significantly high odds ratio (OR = 3.4). DNA sequencing chromatographs showed a clear heterozygous mutation (c.1226 A>G) (Fig. S1B).

iPS Cell-derived mDA Neurons are Enriched Using a Combination of Cell Surface Markers

Next, we investigated potential molecular mechanisms responsible for PD in dopaminergic neurons derived from fibroblasts of the affected twin, unaffected twin, a subject with sporadic PD, and four healthy subjects (Table S1). We used Sendai virus reprogramming to generate transgene-free iPS cell lines, all well characterized in Figure S2A–G.

Utilizing the neuronal differentiation protocol (Kriks et al., 2011), we produced mDA progenitors and mDA neurons from the iPS cell lines listed above. After the 11-day differentiation, most cells expressed SOX1 (mDA progenitors marker), FOXA2, and LMX1 (midbrain markers) (Fig. S2H). Further neuronal differentiations gave rise to substantia nigra (A9) dopaminergic neurons by expression of TUJ1 (pan-neuronal marker), TH (DA

neuronal marker), and GIRK2 (A9 neuronal marker). In patch-clamp recordings, iPS cell-derived neurons fired action potentials in response to injected current, exhibiting voltage-gated sodium and potassium currents (Fig. S2I), and also showed spontaneous firing (Fig. S2J), suggesting that these mDA neurons were physiologically active.

Differentiated cultures yield 5–15% mDA neurons (Salti et al., 2013). When characterizing lines, this low yield seemed to exaggerate phenotypic differences. To overcome this problem, we developed an approach to generate midbrain neuron-enriched preparations by fluorescence-activated cell sorting (FACS). Using a combination of surface markers specific to iPS cells, mDA progenitors, and neurons (Pruszak et al., 2007; Yuan et al., 2011), we isolated mDA progenitors on differentiation day 11 and mDA neurons after day 30 (Fig. 1B). Prior to FACS, differentiated culture contained 10–20% cells with neuronal identity (Fig. 1C). Through capture of CD56$^+$/CD133$^+$ double-positive cells, the sample was enriched to contain ~90% mDA progenitors expressing SOX1, SOX2, NESTIN, FOXA2, and LMX1 (data not shown). Through isolation of CD56$^+$/CD24$^+$/CD15$^-$/CD184$^-$ cells, the purity of dopaminergic neurons was increased to ~80%, as identified by expression of TUJ1 and TH. Most importantly, the degree of neuronal enrichment was similar across different cell lines (Fig. 1D, E). Post sorting, mDA-related genes of FOXA2, LMX1, TUJ1, TH, GIRK2, and PITX3 were significantly higher than those of iPS cells, mDA precursors, and unsorted neurons, indicating an efficient enrichment for mDA population (Fig. 1F). These sorted neurons expressed TUJ1, TH, FOXA2, LMX1, and PITX3 on day 36 (Fig 1G). They were maintained for up to 120 days, still expressing A9 neuronal marker, GIRK2 (Fig 1H). This protocol allowed us to perform biochemical and functional analysis on enriched human dopaminergic neurons at uniform purity.

GBA N370S Increases α-synuclein Levels in iPS Cell-derived mDA Neurons

Mitochondrial abnormalities have been increasingly implicated in the pathogenesis of PD, and have been specifically reported in the mouse model of Gaucher disease (Osellame et al., 2013) and dopaminergic neurons with PD-related genetic mutations (Park et al., 2006; Wood-Kaczmar et al., 2008). Using transmission electron microscopy (TEM), we found that mitochondria in all differentiated neurons, including *GBA* N370S mutant mDA neurons, displayed normal morphology and regular distribution in cytoplasm and processes (Fig. S3A). There were no significant differences in cell death in the absence or presence of oxidative stressors (i. e. rotenone, Fig. S3B–C). In the high-resolution, time-lapse video, the neurite outgrowth rates of both twin's neurons were similar. (Fig. S3D)

FAC-sorted neurons with a heterozygous *GBA* N370S displayed reduced GBA protein levels (Fig. 2A, B) and ~50% GCase activity (Fig. 2C) compared to the controls and PD patient-derived neurons without *GBA* mutation. These results are similar to the findings in postmortem PD human brains carrying heterozygous *GBA* mutations (Gegg et al., 2012). *GBA* mutations lead to α-synuclein accumulation (Mazzulli et al., 2011), which prompted us to investigate α-synuclein levels in our cohorts. Consistent with prior work, α-synuclein was not detectable in fibroblasts. Fibroblast progeny, including iPS cells and mDA progenitors, expressed α-synuclein. There were no differences between the monomeric form of α-synuclein across the cell lines (Fig. 2D). Interestingly, when differentiated into mDA

neurons, cell lines harboring *GBA* N370S had significantly higher α-synuclein levels regardless of disease status (Fig. 2E), suggesting that *GBA* N370S perturbs α-synuclein processing. In contrast, α-synuclein mRNA level did not differ in these cell lines (Fig. 2F), indicating that the *GBA* mutation did not interfere with α-synuclein transcription. Overall, dopaminergic neurons from both twins with *GBA* N370S mutation had higher α-synuclein immunoreactivity in the cell body than the healthy control. In addition, slightly greater α-synuclein expression was observed in the neurites of dopaminergic neurons from the affected compared to the unaffected twin (Fig. 2G, H). All these findings support the theory that *GBA* N370S may lead to α-synuclein accumulation.

Genetic and Non-genetic Factors Contribute to DA Levels in Dopaminergic Neurons

We speculated that PD iPS cell-derived mDA neurons had an impaired capacity to synthesize and release DA. To test this, we performed high-performance liquid chromatography (HPLC) to measure the intra- and extracellular levels of both DA and 3,4-dihydroxyphenylacetic acid (DOPAC, an MAO-dependent metabolite of DA). The chromatograph peaks of DA and DOPAC in iPS cell-derived mDA neurons were confirmed by matching the retention times of known standards (Fig. 3A, B). L-DOPA (100 μM, 30-min treatment) significantly increased DA production, indicating that iPS cell-derived mDA neurons quickly converted L-DOPA into DA, which was then released (Fig. 3C). The graph indicated that iPS cell-derived dopaminergic neurons from the *GBA*-mutated unaffected twin showed reduced DA production compared to the well-characterized control (C1). In addition, dopaminergic neurons from the affected twin and the sporadic PD patient displayed lower intra- and extracellular DA levels (left panels of Fig. 3D and Fig. S4A–B). Surprisingly, another subject (C2)—with a family history of PD—had reduced DA levels, suggesting this patient has the potential to develop PD, despite the absence of known genetic PD mutations. To rule out that the control subject's (C2) DA level was due to technical variation, we included iPS cell lines from two additional healthy control subjects (C3 and C4) without a family history of PD. The two controls produced very similar intra- (6 fmol/μg) and extracellular DA (6 fmol/μl) and displayed comparable DA:DOPAC ratios as C1 (Fig. S4C).

Further investigation revealed the total-DA:total-DOPAC ratio was lower in dopaminergic neurons from PD cases than controls. The ratio was notably lower in the affected twin and the sporadic PD case, indicating elevated MAO activity. Ratios in all unaffected samples, including C2, were similar (right panels of Fig. 3D and Fig. S4A–B).

In addition to the single-cell patch clamp technique, population-level electrical activity was measured using multi-electrode arrays (MEAs). Spontaneous activity (isolated single spikes, and multiple-spike bursts) was evident in cultures of neurons by day 30 (**Fig. 3E1**). Spontaneous activity in mDA neurons from the affected twin was significantly lower when expressed as either well-wide spike rate or the number of active electrodes per well (**Fig. 3E2–3**), which could arise from either a cell-autonomous deficiency in excitability, or a lack of synaptic drive from neighboring cells. By day 52, mDA neurons from the unaffected twin developed robust synchronous bursting patterns indicative of maturing neuronal networks. Although the firing rate of mDA neurons from the affected twin increased between days 30

and 52, no synchrony emerged over this period (**Fig. 3E2–3**). Taken together, these results illustrate a delay in the emergence of spontaneous action potentials, and an absence—or delay to times beyond the course of this experiment—of synchronous activity in the affected twin.

RNA-Seq Reveals that Elevated MAO-B might Play a Role in DA Regulation

To explore the pathogenic factors that may explain the clinical Parkinsonism in the affected twin, we investigated the global transcriptome of iPS cells. RNA-seq analysis showed that there were no differentially expressed genes between healthy and diseased iPS cell lines, displaying non-hierarchical clustering (Fig. S5A). Next, we examined the global gene expression profiling in FAC-sorted neurons. All R2 correlations between biological replicates were over 0.9, indicating experimental reproducibility. Looking into the RNA-seq data for more details on 20 glial genes, we found the canonical glial markers showed very low expression throughout all 14 iPS cell-derived neuronal samples (Fig. S5B), suggesting a consistence of neuronal purification without glial cell contamination.

We initially characterized the expression differences in mDA neurons from all PD cases (6 independent samples) and controls (8 independent samples), identifying 1,028 differentially expressed genes making up the PD expression signature. Strikingly, *MAOB* gene was identified as significantly differentially expressed (p = 0.046). The heat map clearly differentiates cases from controls, where interestingly most differentially expressed genes had lower expression in PD cases compared to controls (Fig. 4A). In the clustering, the RNA expression pattern of the control (C2) with a family history of PD located close to the PD expression signature suggested a susceptibility to PD (Fig. 4A).

To elucidate expression differences between twins, we specifically focused on genes involved in DA synthesis, storage, release/uptake, and PD pathogenesis. As seen in Figure 4B, upregulated *MAOB* gene expression (+ 4.19-fold, p=0.0385) stood out in the set with an arbitrary 2-fold change cutoff. We confirmed the presence of elevated levels of *MAOB* mRNA (Fig. 4C) and MAO-B protein (Fig. 4D) in neurons from the affected twin. These data suggest that abnormally high *MAOB* expression, an additional risk factor to the vulnerable twin, potentially contributed to the onset of PD in the affected twin.

Over-expression of GBA Rescues α-synuclein Phenotype and, together with MAO-B Inhibitor, Promotes DA Production

To investigate the specificity of *GBA* mutation on α-synuclein level, we over-expressed GBA to compensate for the deficiency of GBA in the dopaminergic neurons from both twins by lentivirus infection. Prior to this, we validated the lentivirus 7.2 wild-type *GBA*, expressing V5 tag and GBA, and ensured its high infection efficiency in FAC-sorted mDA neurons. Three days post-infection, nearly all TH-positive mDA neurons co-expressed GBA. A remarkable increase of GBA immunoreactivity was observed in infected cells, but not in the negative control (Fig. 5A). WT GBA overexpression lowered α-synuclein levels in the *GBA* N370S twins-derived neurons (Fig. 5B). Concurrently, GBA enzymatic activities could be significantly rescued compared to un-infected neurons (Fig. 5C).

Reduced DA level is implicated in *GBA* mutants regardless of disease status, especially in PD cases (Fig. 3D), indicating both genetic and non-genetic effects play a role in DA regulation. We treated twins' mDA neurons with Rasagiline (MAO-B inhibitor, 20 μM, 24-hour incubation) or WT GBA lentivirus, and observed a slight increase in extracellular DA production in the affected twin (data now shown). Encouragingly, the combination of transducing lentivirus carrying WT *GBA* and adding Rasagiline could elevate DA levels and decrease DOPAC levels in affected twin's neurons, similar to the levels of the unaffected twin. Elevated DA:DOPAC ratios indicated that Rasagiline inhibited MAO-B enzymatic activity (Fig. 5D). It appeared that WT GBA and Rasagiline independently did not alter DA level in the unaffected twin's neurons. These data suggest the complexity of the mechanisms involved in the rescue experiment.

DISCUSSION

PD pathogenesis is complex; successful disease-modifying treatments will require stratification of genetic and non-genetic factors. In this proof-of-principle study, iPS cell-derived mDA neurons represent individual human nerve cells, recapitulate some key PD pathological features, particularly DA deficiency, and provide a useful strategy to develop disease-modifying remedies.

α-synuclein Accumulation and *GBA* Mutations

Our discoveries suggest that *GBA* N370S interferes with α-synuclein clearance. Interestingly, mutated GBA has previously been shown to cause endoplasmic reticulum stress and autophagic dysfunctions leading to insufficient α-synuclein turnover (Cullen et al., 2011). In postmortem analysis of PD brains with *GBA* mutations, Lewy bodies are immunoreactive for GBA, suggesting that GBA mutations are sufficient for α-synuclein aggregation (Goker-Alpan et al., 2010).

α-synuclein aggregation is a pathological hallmark of PD. Accumulating evidence has identified this phenotype in dopaminergic neurons derived from genetic PD patients with *SNCA* triplications, *GBA* N370S/84GG, truncated *PARKIN*, *LRRK2* G2019S, and *SNCA* A53T (Devine et al., 2011; Imaizumi et al., 2012; Mazzulli et al., 2011; Nguyen et al., 2011; Ryan et al., 2013; Sanchez-Danes et al., 2012). Although we did not observe differences in the α-synuclein levels between twins harboring *GBA* N370S, more α-synuclein was found in the neurites of the affected twin. This could be due to epigenetic changes of genes regulating cytoskeletal networks that interfere with α-synuclein trafficking (Freundt et al., 2012). Consistent with the previous reports on DA neurons with *GBA* mutations, we observed an increase in monomeric α-synuclein levels; however, we did not discover α-synuclein aggregation. In the Gaucher disease model, neurons with GBA compound heterozygous mutations N370S/84GG displayed less than 10% GCase activity. In contrast, neurons derived from twins carrying heterozygous *GBA* N370S exhibited an approximately 50% decrease in GCase activity. Therefore, the severe GBA enzymatic deficiency may be required for α-synuclein aggregation. This scenario was reinforced in the animal model, in which homozygous *GBA* mutations enhanced α-synuclein aggregations in mouse brains

(Sardi et al., 2011). This implies that additional factors are important for the synucleinopathy in PD brains carrying heterozygous *GBA* mutations.

DA Homeostasis Defects in Neurons from PD Patients

Dopaminergic neurons with *Parkin* deletions showed enhanced DA release, and maintained the endogenous DA levels (Jiang et al., 2012). In contrast, neurons with *LRRK2* G2019S mutation demonstrated reduced DA release (Nguyen et al., 2012). These results suggest that PD-related gene mutations might play different roles in DA homeostasis. In our study, mDA neurons carrying *GBA* N370S showed reduced DA levels, similar to prior findings of DA neurons with *LRRK2* G2019S. How *GBA* mutations cause reduced DA levels is poorly understood. One possibility is that reduced DA release is secondary to increased α-synuclein levels. α-synuclein plays a pivotal role in synaptic vesicle regulation, and overexpressing α-synuclein inhibited DA release by 70–80% in mouse nigral neurons (Lundblad et al., 2012).

Intriguingly, we found different DA levels between twins discordant for PD, suggesting that non-genetic factors could further perturb DA homeostasis in addition to *GBA* mutations. RNA-seq data indicated that *MAOB* was highly expressed in the affected twin, resulting in an overall decrease in DA levels and a lower DA:DOPAC ratio. MAO-B inhibition has been postulated to be disease-modifying in PD. A clinical trial of a MAO-B inhibitor, Rasagiline, has shown promising results on slowing PD progression (Olanow et al., 2009). It is still unclear how MAO-B level is upregulated in the affected twin. In schizophrenia, a neuropsychiatric disorder linked to DA dysregulation, hyper-methylation of CpG sites of MAOs have been found in the postmortem brains of patients (Yang et al., 2012). Further research on the methylation patterns of CpG sites of MAOs is required to elucidate the epigenetic changes in the affected twin. Using iPS cell-derived neurons to study epigenetic alterations has drawbacks since the reprogramming process is mostly an epigenetic event and aberrant methylation patterns could occur during the reprogramming and differentiation processes. Despite this caveat, the disease-relevant epigenetic regulations are conserved during the neuronal differentiation in the classical epigenetic neurological disorders (Chamberlain et al., 2010; Yang et al., 2010). In addition, MAO up-regulation has also been found in dopaminergic neurons from PD patients, suggesting that increased MAO could be a common stress-response in PD but may also be directly linked to defective DA regulation.

Improved Neuronal Purification as a Key Step to Cellular Phenotypes

Reliable production of homogeneous mDA neurons is paramount to mechanistic studies and cell-based therapies in PD. Creating reporter transgenic lines has been proposed as a strategy for mDA neuron enrichment (Ganat et al., 2012), but there is no consensus on the best promoter, and a gene knock-in can also potentially disrupt the recipient's genome. Given those specific cell surface markers indicative of developmental stage and lineage specification (Pruszak et al., 2007), a combination of cell surface signatures permits isolation of mDA progenitors and neurons from the differentiated mixture. The combination of CD184^{+}/CD271^{−}/CD44^{−}/CD24^{+} enables the isolation of mDA progenitors, and CD184^{−}/CD44^{−}/CD15[LOW]/CD24^{+} defines the cell surface marker signature for the purification of neurons (Yuan et al., 2011). We isolated CD56^{+}/CD24^{+}/CD15^{−}/CD184^{−} population and

achieved 80% purity of mDA neurons, thereby allowing us to perform reliable biochemical and physiological analysis.

EXPERIMENTAL PROCEDURES

Subjects, Genotyping, and Whole-exome Sequencing

Seven subjects—a man with a five-year history of PD (PD-1, 2), his MZ twin brother without PD, one sporadic PD patient (Sporadic PD-1), and four healthy subjects (C1, C2, C3, and C4)—were recruited for this study (Table S1). DNA from their fibroblasts was extracted for genotyping and whole exome sequencing. See Supplemental Information for more details. Studies were approved by and performed in accordance with the Western IRB and NYU School of Medicine IRBs.

Transgene-free iPS Cell Generation, Maintenance, and Characterization

Using CytoTune® iPS Sendai reprogramming protocol, we converted fibroblasts into transgene-free iPS cells. See Supplemental Information for more details on iPS cell generation, maintenance, and characterization.

Midbrain Neuronal Differentiation and Characterization

The differentiation procedure consists of 11-day neural induction and DA neuronal pattering, as described previously (Kriks et al., 2011). See Supplemental Information for more details.

Electrophysiology and Multi-electrode Array Recordings

Whole-cell patch clamp was performed on neurons plated on 13mm plastic coverslips (Thermanox, Thermo) from days 50–56. Both twins' neurons from day 30 and day 52 were plated in 4 wells each of a 12-well MEA plate from Axion Biosystems. See Supplemental Information for full details.

See Supplemental Information for full details regarding Immunohistochemistry and Western blot, Fluorescence-activated Cell Sorting, Transmission Electron Microscopy, High-performance Liquid Chromatography, RNA-Seq, Real-time PCR Assay and GBA-lentiviral Infection.

Statistical Analysis

Statistical analysis was performed using GraphPad Prism v6.0. Data are described as Mean ± SEM. Student's t-test was designed for the comparison of two groups. One-way analysis of variance (ANOVA) was applied for multiple comparisons. The result was considered statistically significant when $P < 0.05$, 0.01 or 0.001.

Supplementary Material

Refer to Web version on PubMed Central for supplementary material.

Acknowledgments

References

Anheim M, Elbaz A, Lesage S, Durr A, Condroyer C, Viallet F, Pollak P, Bonaiti B, Bonaiti-Pellie C, Brice A, et al. Penetrance of Parkinson disease in glucocerebrosidase gene mutation carriers. Neurology. 2012; 78:417–420. [PubMed: 22282650]

Chamberlain SJ, Chen PF, Ng KY, Bourgois-Rocha F, Lemtiri-Chlieh F, Levine ES, Lalande M. Induced pluripotent stem cell models of the genomic imprinting disorders Angelman and Prader-Willi syndromes. Proc Natl Acad Sci U S A. 2010; 107:17668–17673. [PubMed: 20876107]

Cooper O, Seo H, Andrabi S, Guardia-Laguarta C, Graziotto J, Sundberg M, McLean JR, Carrillo-Reid L, Xie Z, Osborn T, et al. Pharmacological rescue of mitochondrial deficits in iPSC-derived neural cells from patients with familial Parkinson's disease. Sci Transl Med. 2012; 4:141ra190.

Cullen V, Sardi SP, Ng J, Xu YH, Sun Y, Tomlinson JJ, Kolodziej P, Kahn I, Saftig P, Woulfe J, et al. Acid beta-glucosidase mutants linked to Gaucher disease, Parkinson disease, and Lewy body dementia alter alpha-synuclein processing. Ann Neurol. 2011; 69:940–953. [PubMed: 21472771]

Devine MJ, Ryten M, Vodicka P, Thomson AJ, Burdon T, Houlden H, Cavaleri F, Nagano M, Drummond NJ, Taanman JW, et al. Parkinson's disease induced pluripotent stem cells with triplication of the alpha-synuclein locus. Nat Commun. 2011; 2:440. [PubMed: 21863007]

Do CB, Tung JY, Dorfman E, Kiefer AK, Drabant EM, Francke U, Mountain JL, Goldman SM, Tanner CM, Langston JW, et al. Web-based genome-wide association study identifies two novel loci and a substantial genetic component for Parkinson's disease. PLoS Genet. 2011; 7:e1002141. [PubMed: 21738487]

Freundt EC, Maynard N, Clancy EK, Roy S, Bousset L, Sourigues Y, Covert M, Melki R, Kirkegaard K, Brahic M. Neuron-to-neuron transmission of alpha-synuclein fibrils through axonal transport. Ann Neurol. 2012; 72:517–524. [PubMed: 23109146]

Ganat YM, Calder EL, Kriks S, Nelander J, Tu EY, Jia F, Battista D, Harrison N, Parmar M, Tomishima MJ, et al. Identification of embryonic stem cell-derived midbrain dopaminergic neurons for engraftment. J Clin Invest. 2012; 122:2928–2939. [PubMed: 22751106]

Gegg ME, Burke D, Heales SJ, Cooper JM, Hardy J, Wood NW, Schapira AH. Glucocerebrosidase deficiency in substantia nigra of parkinson disease brains. Ann Neurol. 2012; 72:455–463. [PubMed: 23034917]

Goker-Alpan O, Stubblefield BK, Giasson BI, Sidransky E. Glucocerebrosidase is present in alpha-synuclein inclusions in Lewy body disorders. Acta Neuropathol. 2010; 120:641–649. [PubMed: 20838799]

Imaizumi Y, Okada Y, Akamatsu W, Koike M, Kuzumaki N, Hayakawa H, Nihira T, Kobayashi T, Ohyama M, Sato S, et al. Mitochondrial dysfunction associated with increased oxidative stress and alpha-synuclein accumulation in PARK2 iPSC-derived neurons and postmortem brain tissue. Mol Brain. 2012; 5:35. [PubMed: 23039195]

Jiang H, Ren Y, Yuen EY, Zhong P, Ghaedi M, Hu Z, Azabdaftari G, Nakaso K, Yan Z, Feng J. Parkin controls dopamine utilization in human midbrain dopaminergic neurons derived from induced pluripotent stem cells. Nat Commun. 2012; 3:668. [PubMed: 22314364]

Kriks S, Shim JW, Piao J, Ganat YM, Wakeman DR, Xie Z, Carrillo-Reid L, Auyeung G, Antonacci C, Buch A, et al. Dopamine neurons derived from human ES cells efficiently engraft in animal models of Parkinson's disease. Nature. 2011; 480:547–551. [PubMed: 22056989]

Lill CM, Roehr JT, McQueen MB, Kavvoura FK, Bagade S, Schjeide BM, Schjeide LM, Meissner E, Zauft U, Allen NC, et al. Comprehensive research synopsis and systematic meta-analyses in

Parkinson's disease genetics: The PDGene database. PLoS Genet. 2012; 8:e1002548. [PubMed: 22438815]

Lundblad M, Decressac M, Mattsson B, Bjorklund A. Impaired neurotransmission caused by overexpression of alpha-synuclein in nigral dopamine neurons. Proc Natl Acad Sci U S A. 2012; 109:3213–3219. [PubMed: 22315428]

Marder KS, Tang MX, Mejia-Santana H, Rosado L, Louis ED, Comella CL, Colcher A, Siderowf AD, Jennings D, Nance MA, et al. Predictors of parkin mutations in early-onset Parkinson disease: the consortium on risk for early-onset Parkinson disease study. Arch Neurol. 2010; 67:731–738. [PubMed: 20558392]

Mazzulli JR, Xu YH, Sun Y, Knight AL, McLean PJ, Caldwell GA, Sidransky E, Grabowski GA, Krainc D. Gaucher disease glucocerebrosidase and alpha-synuclein form a bidirectional pathogenic loop in synucleinopathies. Cell. 2011; 146:37–52. [PubMed: 21700325]

Nguyen HN, Byers B, Cord B, Shcheglovitov A, Byrne J, Gujar P, Kee K, Schule B, Dolmetsch RE, Langston W, et al. LRRK2 mutant iPSC-derived DA neurons demonstrate increased susceptibility to oxidative stress. Cell Stem Cell. 2011; 8:267–280. [PubMed: 21362567]

Olanow CW, Rascol O, Hauser R, Feigin PD, Jankovic J, Lang A, Langston W, Melamed E, Poewe W, Stocchi F, et al. A double-blind, delayed-start trial of rasagiline in Parkinson's disease. N Engl J Med. 2009; 361:1268–1278. [PubMed: 19776408]

Osellame LD, Rahim AA, Hargreaves IP, Gegg ME, Richard-Londt A, Brandner S, Waddington SN, Schapira AH, Duchen MR. Mitochondria and quality control defects in a mouse model of Gaucher disease--links to Parkinson's disease. Cell Metab. 2013; 17:941–953. [PubMed: 23707074]

Park J, Lee SB, Lee S, Kim Y, Song S, Kim S, Bae E, Kim J, Shong M, Kim JM, et al. Mitochondrial dysfunction in Drosophila PINK1 mutants is complemented by parkin. Nature. 2006; 441:1157–1161. [PubMed: 16672980]

Pruszak J, Sonntag KC, Aung MH, Sanchez-Pernaute R, Isacson O. Markers and methods for cell sorting of human embryonic stem cell-derived neural cell populations. Stem Cells. 2007; 25:2257–2268. [PubMed: 17588935]

Reinhardt P, Schmid B, Burbulla LF, Schondorf DC, Wagner L, Glatza M, Hoing S, Hargus G, Heck SA, Dhingra A, et al. Genetic correction of a LRRK2 mutation in human iPSCs links parkinsonian neurodegeneration to ERK-dependent changes in gene expression. Cell Stem Cell. 2013; 12:354–367. [PubMed: 23472874]

Ryan SD, Dolatabadi N, Chan SF, Zhang X, Akhtar MW, Parker J, Soldner F, Sunico CR, Nagar S, Talantova M, et al. Isogenic human iPSC Parkinson's model shows nitrosative stress-induced dysfunction in MEF2-PGC1alpha transcription. Cell. 2013; 155:1351–1364. [PubMed: 24290359]

Salti A, Nat R, Neto S, Puschban Z, Wenning G, Dechant G. Expression of early developmental markers predicts the efficiency of embryonic stem cell differentiation into midbrain dopaminergic neurons. Stem Cells Dev. 2013; 22:397–411. [PubMed: 22889265]

Sanchez-Danes A, Richaud-Patin Y, Carballo-Carbajal I, Jimenez-Delgado S, Caig C, Mora S, Di Guglielmo C, Ezquerra M, Patel B, Giralt A, et al. Disease-specific phenotypes in dopamine neurons from human iPS-based models of genetic and sporadic Parkinson's disease. EMBO Mol Med. 2012; 4:380–395. [PubMed: 22407749]

Sardi SP, Clarke J, Kinnecom C, Tamsett TJ, Li L, Stanek LM, Passini MA, Grabowski GA, Schlossmacher MG, Sidman RL, et al. CNS expression of glucocerebrosidase corrects alpha-synuclein pathology and memory in a mouse model of Gaucher-related synucleinopathy. Proc Natl Acad Sci U S A. 2011; 108:12101–12106. [PubMed: 21730160]

Sidransky E, Nalls MA, Aasly JO, Aharon-Peretz J, Annesi G, Barbosa ER, Bar-Shira A, Berg D, Bras J, Brice A, et al. Multicenter analysis of glucocerebrosidase mutations in Parkinson's disease. N Engl J Med. 2009; 361:1651–1661. [PubMed: 19846850]

Tanner CM, Ottman R, Goldman SM, Ellenberg J, Chan P, Mayeux R, Langston JW. Parkinson disease in twins: an etiologic study. JAMA. 1999; 281:341–346. [PubMed: 9929087]

Wirdefeldt K, Gatz M, Reynolds CA, Prescott CA, Pedersen NL. Heritability of Parkinson disease in Swedish twins: a longitudinal study. Neurobiol Aging. 2011; 32:1923, e1921–1928. [PubMed: 21482443]

Wood-Kaczmar A, Gandhi S, Yao Z, Abramov AY, Miljan EA, Keen G, Stanyer L, Hargreaves I, Klupsch K, Deas E, et al. PINK1 is necessary for long term survival and mitochondrial function in human dopaminergic neurons. PLoS One. 2008; 3:e2455. [PubMed: 18560593]

Yang Q, Ikemoto K, Nishino K, Yamaki J, Kunii Y, Wada A, Homma Y, Niwa SI. DNA methylation of the Monoamine Oxidases A and B genes in postmortem brains of subjects with schizophrenia. Open Journal of Psychiatry. 2012; 2:374–383.

Yang Y, Gozen O, Vidensky S, Robinson MB, Rothstein JD. Epigenetic regulation of neuron-dependent induction of astroglial synaptic protein GLT1. Glia. 2010; 58:277–286. [PubMed: 19672971]

Yuan SH, Martin J, Elia J, Flippin J, Paramban RI, Hefferan MP, Vidal JG, Mu Y, Killian RL, Israel MA, et al. Cell-surface marker signatures for the isolation of neural stem cells, glia and neurons derived from human pluripotent stem cells. PLoS One. 2011; 6:e17540. [PubMed: 21407814]
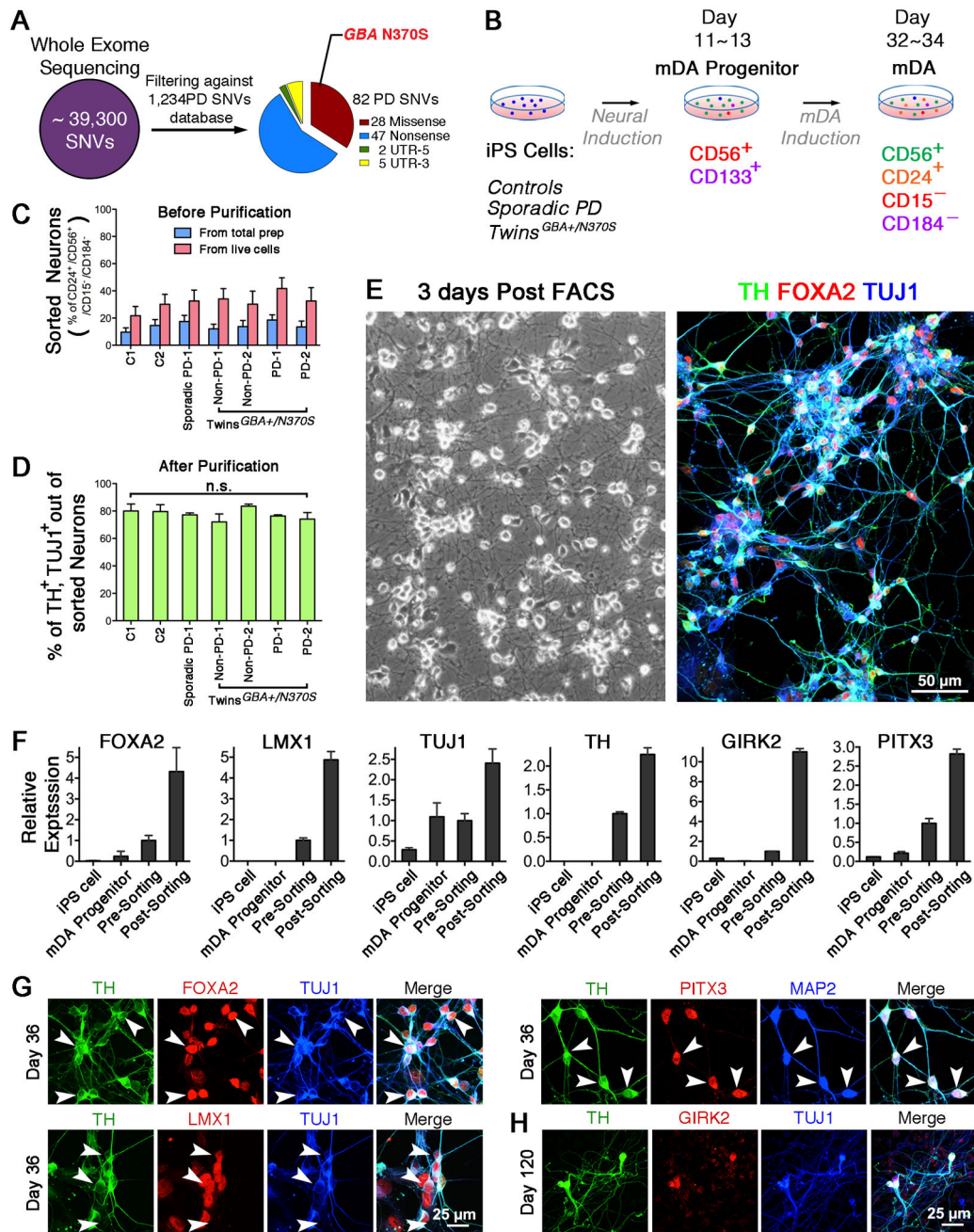
Figure 1. Characterization of FACS-isolated Neurons from a Cohort of iPS Cells
(A) Whole-exome sequencing the fibroblasts derived from twins. (B) Diagram depicts two panels of antibodies at two time points to isolate mDA progenitors and neurons. (C) FACS analysis of the neuronal differentiation before purification (n = 6~11). (D) Percent of TH/TUJ1-positive cells in sorted CD56+/CD24+/CD15−/CD184− population (n.s. = not significant, n = 3). (E) Phase-contrast image of sorted cells 3 days post-FACS, and immunofluorescence of TH, FOXA2 and TUJ1. (F) Quantitative gene expression analysis in iPS cells, mDA procursors, unsorted neurons, and FAC-sorted neurons (n = 3). (G – H)

Immunofluorescence for TH, FOXA2, TUJ1, LMX1, PITX3, MAP2, and GIRK2 to confirm the midbrain dopaminergic lineage on day 36 and 120. Scale bars, 50 μm (E), 25 μm (G, H).
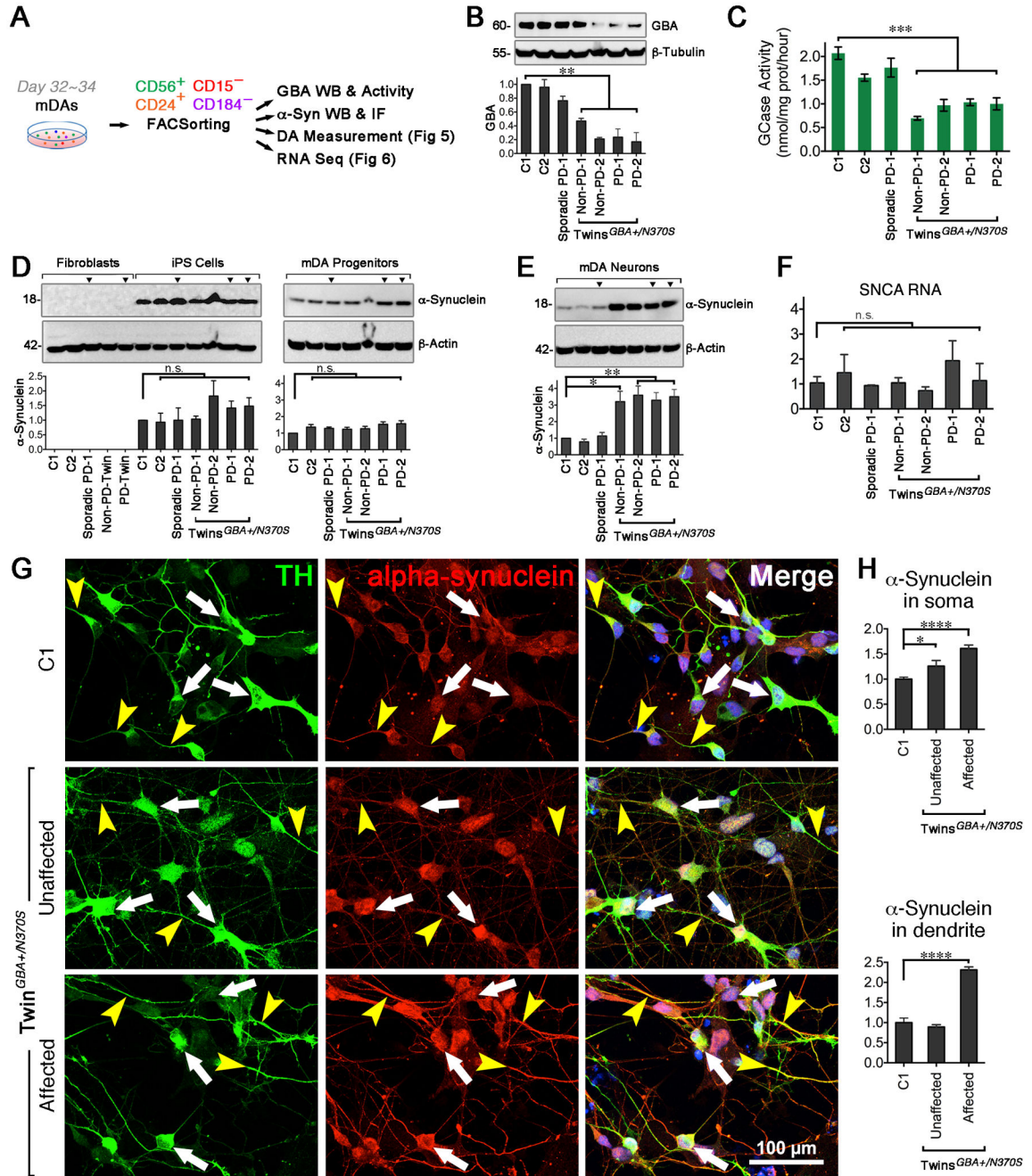
Figure 2. α-synuclein Level is Higher in *GBA* N370S Carrier-derived Neurons
(A) Diagram depicts biochemical assay, immunofluorescence, HPLC, and RNA-seq in FAC-sorted neurons on day 32–34. (B) GBA protein level was lower in twins carrying *GBA* N370S (n = 3). (C) GCase activity (5×10^4 sorts, n = 4) were analyzed at Genzyme Corporation (Boston, MA), ANOVA, *** p < 0.001). (D) α-synuclein protein expression in fibroblasts, iPS cells, and purified mDA progenitors (n.s. = not significant). α-synuclein protein (E) and RNA (F) expression in sorted mDA neurons (ANOVA, * p < 0.05, ** p < 0.01, n.s. = not significant. n = 3). (G – H) Immunofluorescence and quantitation (n ≥ 15

cells, measured for each group) of overall α-synuclein (white arrows) and α-synuclein in the neurites (yellow arrowheads). Scale bar, 100 μm.
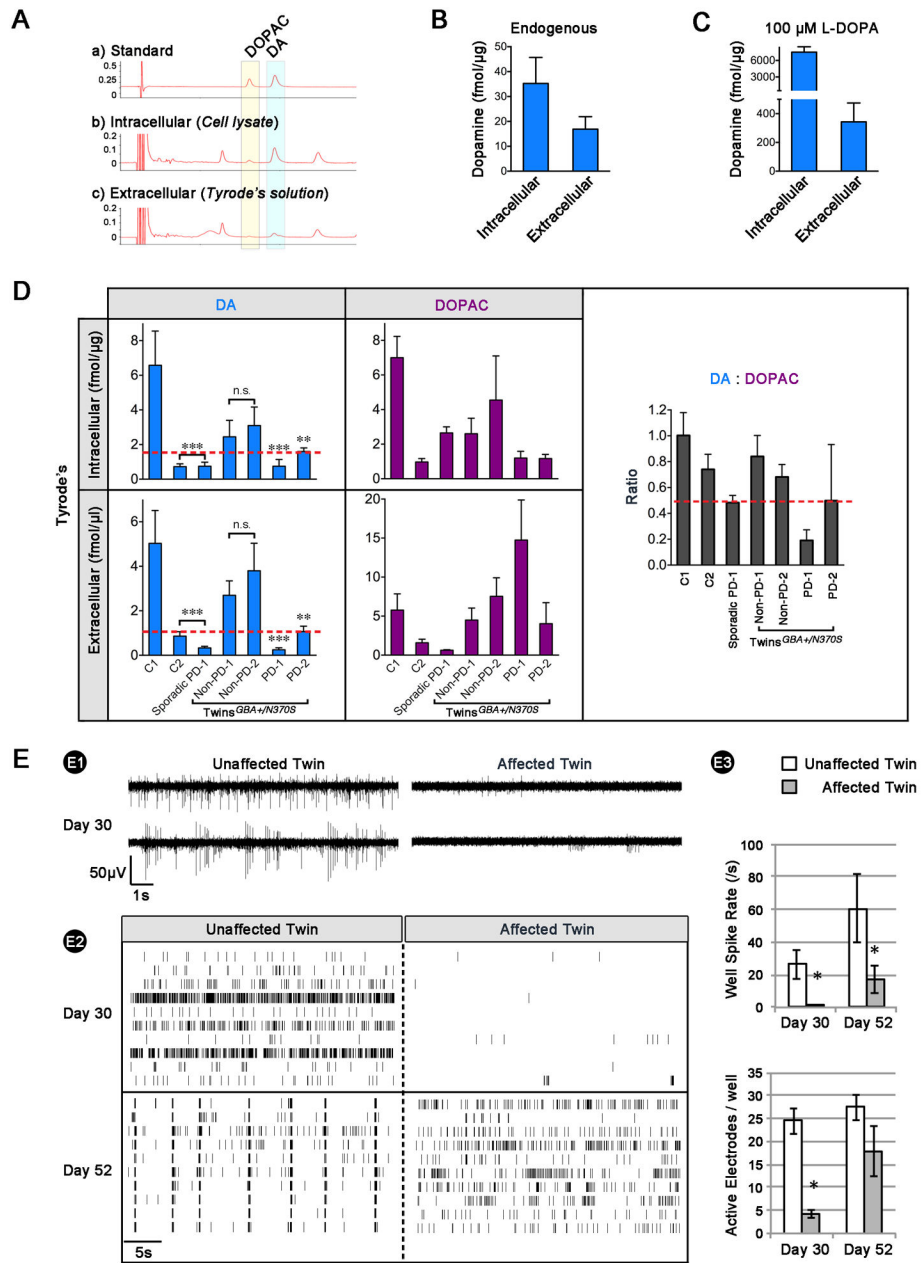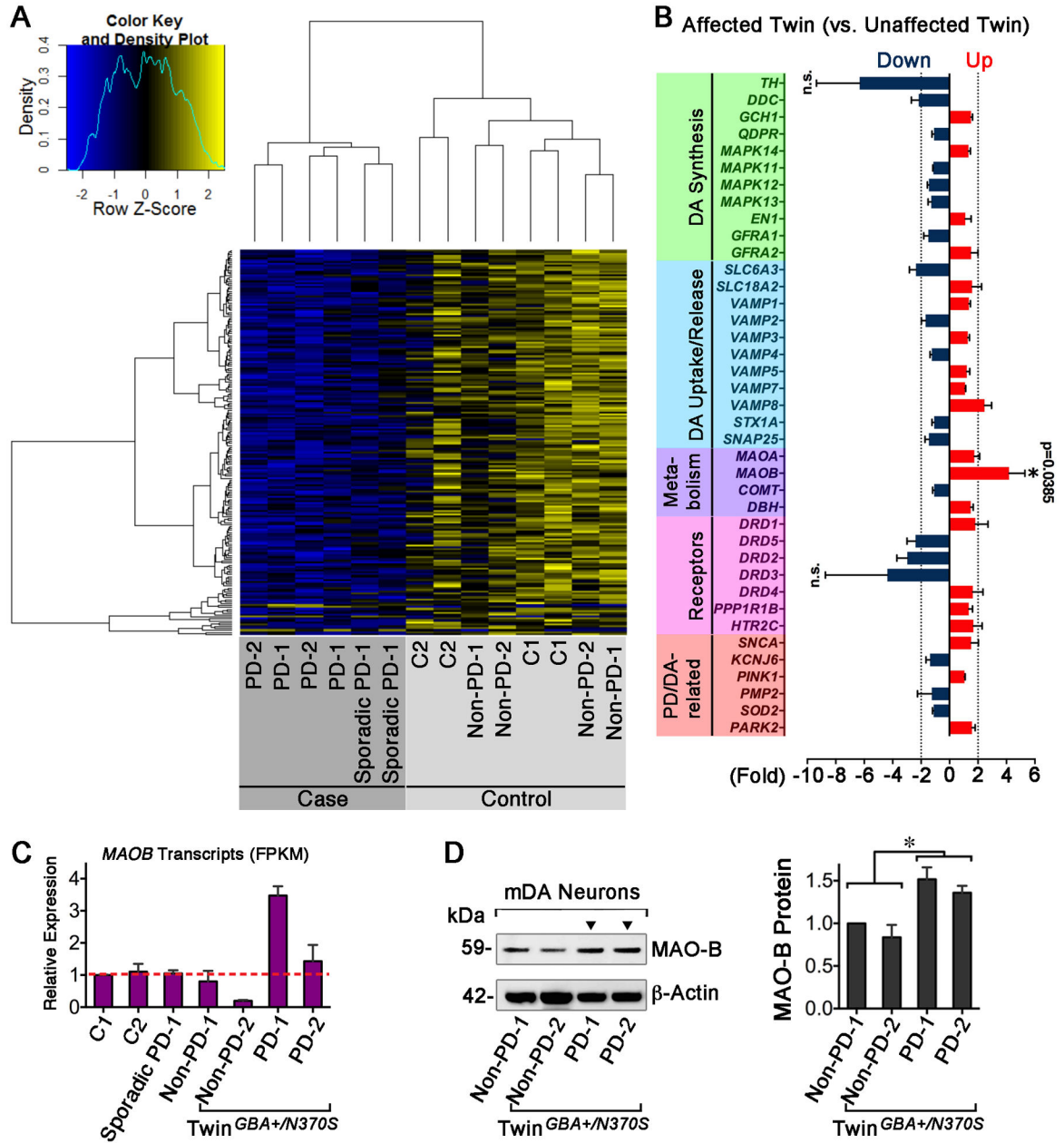
Figure 3. Affected Twin-derived Neurons Present Lower DA Level and Impaired Network Activity

(A) A trace of standard chemicals DA and DOPAC is shown on top for comparison. Representative HPLC traces of cell lysate (indicative of DA and DOPAC synthesis) and Tyrode's buffer (indicative of DA and DOPAC release). Compiled HPLC data of intra- and extracellular DA concentrations before (B) and after supplementing 100 µM L-Dopa (C). (D) Compiled HPLC data showed intra- and extracellular DA (left panels) and DOPAC (middle panels) concentrations between lines and DA:DOPAC (right panel) ratios. The lower DA levels (below the dash red line) suggested a pathologic condition (ANOVA, ** $p < 0.01$, *** $p < 0.001$, n = 3~6). (E) Multi-electrode array in twins. E1) Raw data traces for

two electrodes from a representative well. E2) Spike raster plots on day 30 (top) and 52 (bottom) post-plating. E3) Mean spike rate and number of active electrodes (n = 4, *t*-test; * P < 0.05).

Figure 4. *MAOB* Expression is Elevated in PD-iPS Cell-derived Neurons
(A) Heat map shows the global gene expression patterns of PD neurons differ from those of a healthy control (C1) and the unaffected twin (blue is lower expression and yellow is higher). (B) A list of genes related with DA synthesis, uptake/release, metabolism, receptors and PD/dopaminergic neurons were differentially expressed in twins (dark blue: down-regulation; red: up-regulation). An asterisk indicates significantly higher *MAOB* expression in affected twin (p = 0.0385, n = 4). (C) The transcriptional abundance of *MAOB* across the cohort of patients and controls. (D) Determination of MAO-B protein in twins' neurons (*t*-test, * p < 0.05, n = 3).
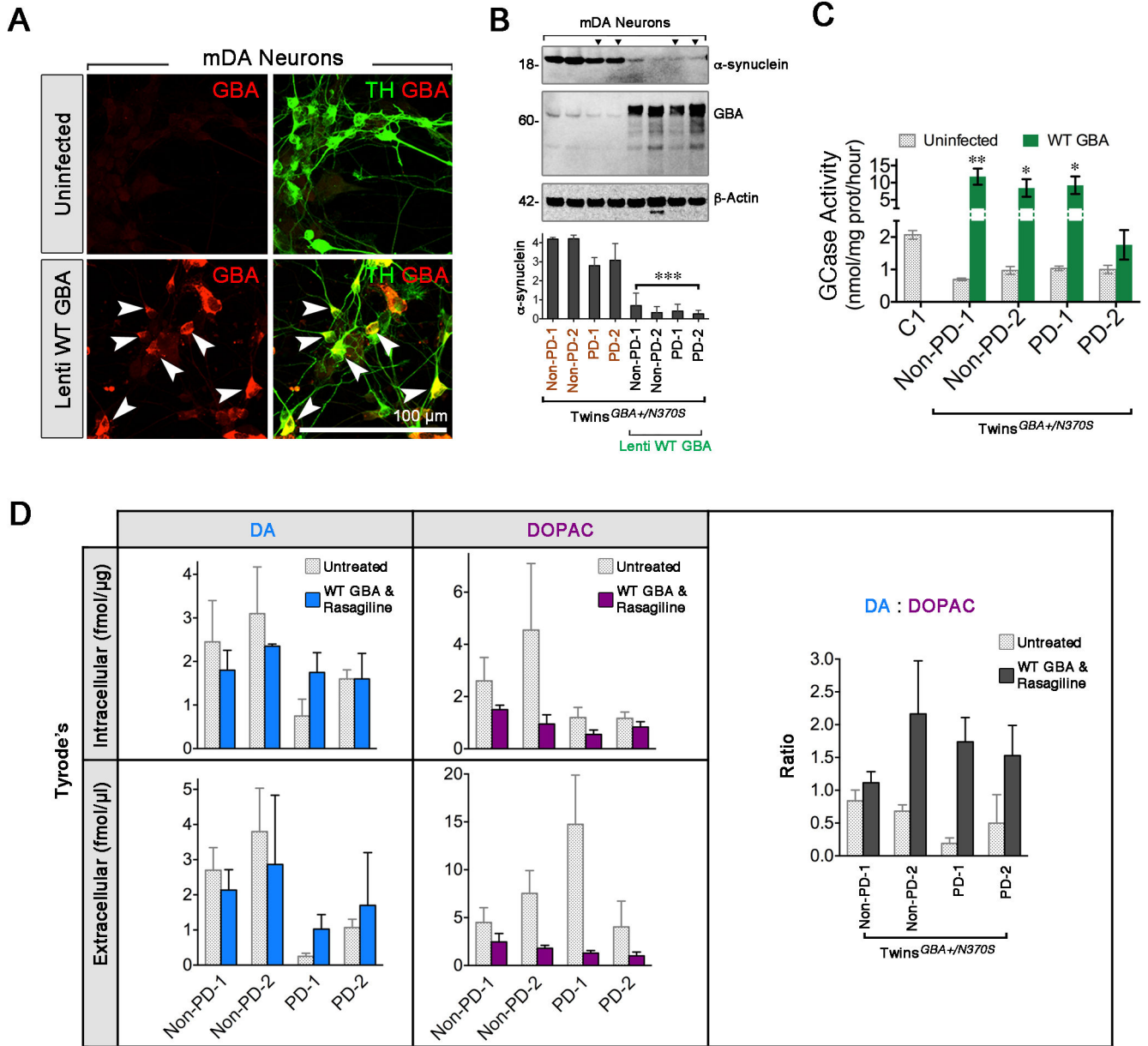
Figure 5. GBA Overexpression Inhibits α-synuclein Level and, together with MAO-B Inhibitor, Rescues DA Deficiency

(A) Validation of the infection and specificity of lentivirus 7.2 WT *GBA* in the dopaminergic neurons stained with TH (green) and GBA (red, arrowheads). (B) Western blot showed GBA overexpression and reduced α-synuclein levels in GBA-infected twins' neurons (*t*-test, *** $p < 0.001$. n = 3). (C) Measurement of GCase activity (grey bars: uninfected cell; green bars: WT GBA. *t*-test, * $p < 0.05$, ** $p < 0.01$. n = 4 biological). (D) HPLC analysis revealed change in DA (left), DOPAC (middle) levels, and DA:DOPAC (right) ratios before (dotted bars) and after GBA infection (solid colorful bars) (n = 3~6). Scale bar, 100 μm.